JOURNAL GEOLOGICAL SOCIETY OF INDIA
Vol.90, August 2017, pp.217-225

Characterization of Fluid Inclusions Encaged in Quartz Veins of Parsoi Formation, Central India

R.K. Dubey* and Ravi Shankar
Department of Applied Geology, India School of Mines, Dhanbad - 826 004, India
E-mail: *rkdbhumin1085@yahoo.co.in*, rkdubey1085@hotmail.com, hunny3011@gamil.com*

ABSTRACT

The study focuses on analysis of primary and secondary fluid inclusions present in quartz veins hosted in the phyllites to explore the stress and temperature conditions at the time of formation of metasediment sequences of the of Parsoi Formation, central India. The results reveal the two-phase liquid-rich fluid inclusions that indicate that the intrusions of quartz veins in phyllite may have taken place between the temperature from 168.8°C to 256.3°C with an average of 205.55°C from a magmatic moderately saline fluid (3.7 to 18.29 wt. % NaCl equiv.). The final ice-melting temperatures ranges from -14.6°C to -2.2°C which indicate that the aqueous fluids are mainly H_2O-NaCl. The density distribution of fluid inclusions rich in liquid H_2O only are unimodel and low in natures and appears to be entrapped between pressure 1.666 to 2.125 kbar at depth of 200m. The study supports epithermal nature of fluid inclusions. The characteristic of fluid inclusions along with lithological and structural peculiarities, nature of structural features may be helpful in exploring the future potential zone of gold mineralization in similar types of area.

INTRODUCTION

Fluid inclusions can be defined as microscopic volume of fluid trapped within crystals at the time of their growth from the mineralized fluid (Roedder and Bodnar, 1980). The fluid inclusions form when crystals grow in presence of a fluid phase, consequently some of the fluid gets trapped as imperfections in the growing crystal (Hollister and Crawford, 1981). The fluid may be in form of liquid, vapor or supercritical fluid having composition essentially of pure water, brines of various salinity, gas or gas bearing liquids, and silicate, sulfide or carbonate melts (Bodnar, 2003). During trapping (at particular P/T) these fluids remains homogeneous in nature that becomes multiphase when cooled at room temperature (Roedder, 1992). The most common phases of such inclusions are vapour and liquid which are results of differential shrinkage of crystal and liquid on cooling (Sorby, 1858). The inclusions can be grouped into three classes based on their origin viz., primary, secondary, and pseudo-secondary (Roedder and Bodnar, 1980). The primary inclusions are formed during formation of the enclosing crystals and get trapped parallel to the crystal faces which generally occur in solitary or isolation (Roedder, 1968). These primary inclusions provide information on the conditions of crystallization of host minerals. The secondary inclusions form along fractures that grow after the formation of the host mineral in the sufficient availability of trap fluid. They generally occur in trails or clusters that often cut across grain boundaries. The pseudo-secondary inclusions form as a result of entrapment of fluids along the fractures which develop during the crystallization of the host mineral (Randive et al., 2014). Therefore, these inclusions occur at trails that end abruptly against grain boundaries. The inclusions provide detailed knowledge of the temperatures of past geological events thus act as a good geothermometer (Bodnar, 2003). Besides, the inclusions also give the elaborat details of composition, salinity, density, P-T history of fluid phases at the time of their trapping (Crawford, 1992). The inclusions having size greater than 2 micrometers are sufficiently large to study with the heating and freezing stage, however there is no upper limit of the size related to natural fluid inclusions (Bodnar, 2003). The size of inclusions bears an inverse relationship with the number of inclusions (Roedder, 1984).

The thermometric studies of inclusions are an important tool for the exploration of hydrothermal ore deposits and for development of genetic models of mineralization. The technique also facilitates the proper understanding related to the process responsible for transportation of metals in solution. The mechanisms of metals deposition helps in development of targets for future exploration. The fluid inclusions occurr in common transparent hydrothermal minerals calcite, fluorite, barite, halite, quartz, etc., moreover, quartz is considered as most suitable mineral for bulk of thermometric study because of its transparency and abundance (Hollister and Crawford, 1981). In addition to these the quartz veins serve as a host for many significant ore deposits of economic importance viz. gold, silver, pyrite, sphalerite, galena, chalcopyrite, and other base metals, etc. The thermometric study of fluid inclusions in quartz veins associated with well-known mineralized zones round the world have been studied by various researchers for establishing their genetic and thermal histories (Morales et al., 1993; O'Hara et al., 1995; Boullier, 1998; Wilkinson, 2001; Kant et al., 2012; Moncada and Bodnar, 2012; Moncada et al., 2012; Tun et al., 2014; Mehrabi et al., 2016). The analysis of these observations provides valuable information about the range and nature of thermometric data from quartz veins of mineralized zones (Table 1). The present work emphasis the general aspects of fluid inclusion and discuss in detail a case study of foliation parallel massive quartz vein intruded in metasediments of Parsoi Formation of Mahakoshal Group. The study area falls between latitude 24°24'–24°29' and longitude 82°51'- 82°58' of toposheet number 63L/15 of Geological Survey of India. The area is situated in the west of the Rihand river and south of Son river in Sonbhadra district of Uttar Pradesh (UP), which is well-connected from Obra by an all-weather motorable road and also linked with Chopan-Singrauli railway line (Fig.1). The terrain is rather hilly with elevation ranging from 183 meters to 442 meters above mean sea level (MSL). The region exhibits characteristic ridge and valley structures, where ENE-WSW trending hard resistant synclinal quartzites form the ridges and undulating phyllites form the valley. The north-north east (NNE) trending Rihand River located in the eastern border of the area is the main drainage system. The Bijul is another perennial river in the area that flows in a general north-easterly direction. Besides, there are numerous smaller *nalas* in the area having same NNE trend and easterly trends. The region has been frequently intruded by quartz veins of various sizes which occur as small mounds or hillocks, and scattered over the area. These veins are mostly trending (N280^o) parallel to the slaty cleavage and schistosity of the country rocks and sometimes in some

0016-7622/2017-90-2-217/$ 1.00 © GEOL. SOC. INDIA | DOI: 10.1007/s12594-017-0702-z

Table 1. Thermometric study of fluid inclusions in mineralized zones of different parts of world

Location	Host Mineral	Th (°C)	Tfim(oC) (°C)	Salinity (wt%NaCl)	Minerals	References
Santa Margarita vein in the Guanajuato Mining District, Mexico	Quartz	184-300	0 to 4	0-5	Ag-Au	Moncada, D. and Bodnar, R.J. (2012)
Sualan prospect, west Java, Indonesia	Quartz	160- 210	-0.1to -3.0	0.35-4.96	Au	Tun et al. (2014)
La Libertad district, Nicaragua	Quartz	169-372	-0.5to -1.7	0.98-2.15	Au-Ag	Morales et al. (1993)
South Eastern Abitibi subprovince (Quebec, Canada)	Quartz	212 to >450	-33 to -6	30.62- 9.21	Au	Boullier et al. (1998)
Osilo (Sardinia), Italy	Quartz	200-270	0.0 to 2.3	0.0-4.1	Au	Simeone and Simmons, (1999)
Soripesa prospect area, Sumbawaisland, Indonesia	Quartz	182-300	-0.93 to -1.88	1.86-3.15	Au	Kant et al. (2012)
Tarom-Hashtjin metallogenic province, Glojeh district, NW Iran	Quartz	170-340	“7.2 to “0.4	0.5-11	silver- and base metal	Mehrabi et al. (2016)
Donaldag old-bearing quartz veins	Quartz	100-380	-40.3 to -2.4	36.40 - 4.02	Au	Chi and Guha, (2011)
Mississippi valley type deposit	Calcite, Dolomite, Fluorite, Quartz, Barite, Sphelarite	50–180	-	15–30	Pb-Zn	Wilkinson (2001)
Irish-type	Calcite, Dolomite, Quartz, Barite, Sphelarite	150–240	-	10–18	Pb-Zn	Wilkinson (2001)
Volcanic associated massive sulphide deposit	Quartz, Barite	80–340	-	1–8	Cu-Zn-Pb-Ag-Au	Wilkinson (2001)
Granitoid associated vein	Quartz, wolframite, Fluorite, Calcite	150–500	-	0–45	Cu-Au	Wilkinson (2001)
Porphyry-copper	Quartz,	200–700	-	0–70	Cu-Ag-Au	Wilkinson (2001)
Epithermal	Quartz, Calcite, Sphelarite	100–300	-	0–12	Au	Wilkinson (2001)
Mesothermal gold	Quartz, Calcite	200–400	-	2–10	Au	Wilkinson (2001)
Creede deposit in Colorado		200–270C,	-	4.9–11.7	Au	Woods et al. (1982)

cases the veins exhibits angular relation also. The frequent occurrence of quartz veins suggest an extensive influx of siliceous solution probably due to hydrothermal activity related to some possible deep seated intrusive activity (Ghosh, 1966). The quartz vein is also associated with sporadic lead mineralization in the form of specks of galena. Therefore, the present study emphases the study of composition, salinity, density, P-T history of these quartz veins for assessing their comprehensive genetic model and evolutionary history. This study may be significant in case of mineralized zones in general and relevant in exploration of such zones in future in particularly in the area and nearby.

Fig.1. Location map of the area.

GEOLOGICAL SETTING

The Paleoproterozoic Mahakoshal Group is an arc-shaped supracrustal belt developed between the southern boundary of Bundelkhand craton and northern margin of Chhotanagpur Granite Gneissic Complex (CGGC) of peninsular Indian shield (Nair et al., 1995). The Mahakoshal Group, previously recognized as Bijawar Group (Iqballudin and Mohgni, 1981; Mathur and Narain, 1981), represents a rift basin type of tectonic setting (Roy, 2008). The belt has an extension of about 500 km which ranges from northeastern part of Jabalpur district in Madhya Pradesh up to the border of Palamau, in Jharkhand states. This region constitutes the northern part of the Central Indian Tectonic Zone (CITZ) (Radhakrishna, 1989; Acharyya and Roy, 2000) and also considered as an integral part of Son-Narmada lineament zone (Ravi Shanker, 1993). The volcano-sedimentary rock sequences of Mahakoshal Group constitute Chitrangi, Agori and Parsoi formations respectively (Nair et al., 1995). Based on the presence of polymictic conglomerate horizon, Kumar (2005), separated Parsoi Formation from the Mahakoshal Group (Roy and Devarajan, 2000). The rock formations of Mahakoshal Group exhibit sheared contact with relatively younger granite-gneisses at its northern margin and granite-gneisses of Chhotanagpur Granite Gneiss Complex (CGGC) at the southern margin. These formations have unconformable relationship with the overlaying rocks of Vindhyan Supergroup. In

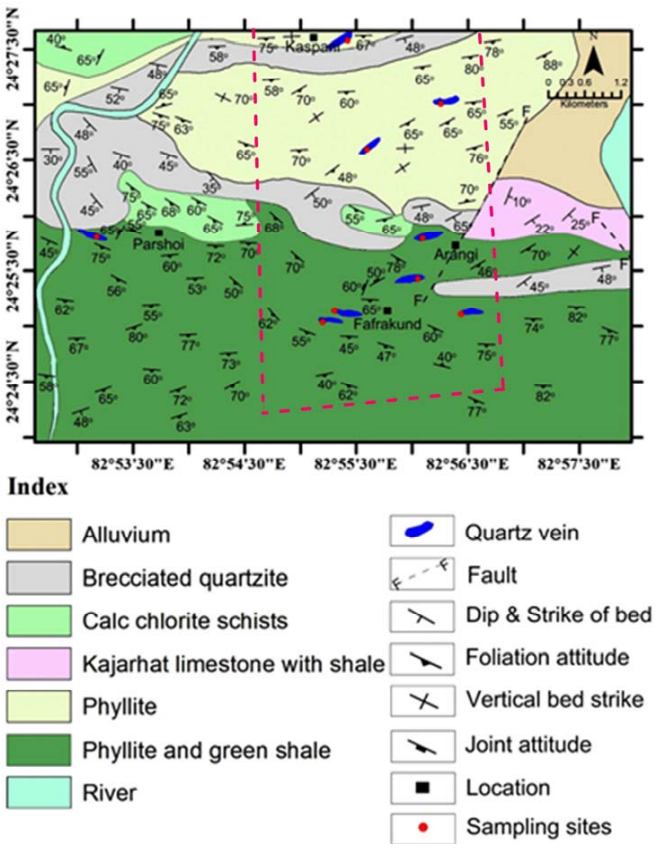

Fig.2. Geological map of study area showing occurrences of Quartz veins.

particular places, the litho units of Mahakoshal Group also exhibit the intrusive contact with rocks of Vindhyan and Gondwana Supergroups. The Parsoi Formation comprises of low grade pelitic metasediments, calc-chlorite-schist, brecciated quartzite, dolomite and siliceous limestone, banded hematite-magnetite-quartzite-chert and jasper with interbedded slate, basic dyke, quartz vein, etc. (Fig.2) (Srivastava 1969). The grayish to grayish green, pinkish or reddish coloured phyllites are thinly bedded exhibiting megascopic characteristic of slaty, phyllitic and at some places schistose structure (Fig.3). The mineral constituents comprise of chlorite, biotite, sericite, fine grained quartz aggregates, and euhedral to subhedral magnetite grains. The dolomitic and silicious limestone comprise of medium sized interlocking grains of dolomite and calcite. These are over-laid by ENE-WSW trending hard resistant grey to greyish white brecciated quartzite forming chains of hillocks and ridges. This youngest brecciated quartzitic unit is showing layered structures with dark bands at some places, and shattered and jointed at another places along with angular fragments of quartz, jasper and chert. Besides quartzite, the small mound and hillocks of quartz veins are found scattered throughout the area (Figs.4-7). The rocks are traversed by number of structural lineaments, joints, foliations and faulting. The phyllitic rocks are showing moderate to high dips which sometimes becomes vertical also at some places. The poles of the foliation and layers of rocks suggest the trend of foliation in ENE and WSW which is almost parallel to the major lineaments viz. Son Narmada north and Son Narmada south faults (trending ENE and WSW) and supports multiple deformation events (Fig.8).

SAMPLES AND METHODOLOGY

Doubly polished wafer thin sections (~ 100 ìm thick) were prepared from 6 samples taken from three different kinds of quartz veins for preliminary petrographic studies and the selection of wafers containing representative population of fluid inclusions. Fluid inclusion

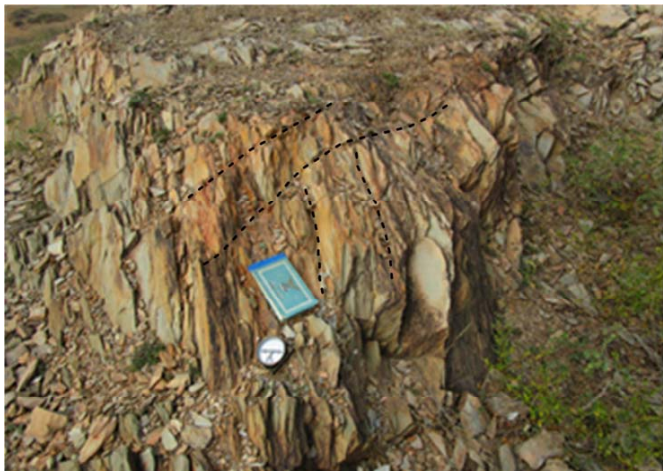

Fig.3. Outcrop of steeply dipping foliated phyllite outcrop near Parsoi village, Sonbhadra, Uttar Pradesh.

assemblages were mapped and classiûed petrographically (after using the criteria of Roedder, 1984 and Goldstein, 2003). The overall morphological features viz. shape, size, degree of fill, spatial relationship, phase within the fluid inclusions were identified on the basis of standard criteria given by Roedder (1984), Bodnar et al., (1985) and Goldstein, (2003). Microthermometric measurements were made by using a Linkam TH MS G-600 heating–freezing stage at the Department of Earth Sciences, Indian Institute of Technology, Bombay, India (Fig.9). The stage has capability of increasing or decreasing temperature over a wide temperature range laying between –200°C and +1500°C (approx.). The stage is attached to high magnification microscope for precisely observing the temperature of phase changes. The stage was calibrated with a series of synthetic fluid inclusions of known compositions. The accuracy was ± 1 ° C below 350°C on heating and ± 0.1°C on freezing. Salinities of liquid rich fluid inclusions were calculated from measured last ice-melting temperatures by using the equation of Hall et al. (1988). The samples namely PR-4 and PR-5 were found containing mostly primary fluid inclusions. The recognized and delineated fluid inclusions were selected for detailed micro-thermometric study. The microthermometric analysis was based on the assumption that the fluid inclusions have not undergone any post-entrapment leakage or necking and also followed a constant density path along the isochore for the system under investigation (e.g. Bodnar, 2003). So, the fluid inclusions exhibiting evidence of necking were excluded for microthermometry. The analysis was begins with cooling the inclusions to lowest temperature with the help of liquid nitrogen, N_2 (freezing temperature, Tf) at which the phase change occurred and was subsequently recorded. Thereafter the temperature was raised up to room temperature and first and final change of phase was observed and recorded carefully. The first change in phase was representing eutectic temperature and final change in phase was representing ice melting temperature (Tfim). These values were used to determine the salinity in case of low saline inclusions (salinity <23.2 wt %) by using the Equation 1 (after Bodnar, 1993)

$$\text{Salinity} = 0.00 + 1.78Q - 0.0442Q^2 + 0.000557Q^3 \qquad (1)$$

where, Q is the freezing point depression (FDI) and salinity in wt% NaCl.

On the basis of the known freezing points of pure H_2O and CO_2, the observed freezing points (Tmf) were substituted in the above equation (Equation 1). The Equation-1 is a kind of equation representing gas law (PV= nRT) equation which directly relates the freezing point depression of the system under observation to the amount of "impurities" present in the system. In addition to above features, it further provides information related to the salinity of the

Fig.4. Massive quartz vein showing its extension near Arangi village, Sonbhadra, Uttar Pradesh.

Fig.5. Outcrop exhibiting highly dipping quartz vein near railway cutting at Arangi locality, Sonbhadra, Uttar Pradesh

Fig.6. Outcrop of quartz vein showing developments of multiple sets of fractures near Fafrakund locality, Sonbhadra, Uttar Pradesh

Fig.7. Outcrop of showing massive quartz vein near Fafrakund locality, Sonbhadra, Uttar Pradesh

fluid. Further the stage was heated from room temperature up to a highest temperature (homogenization temperature, Th) at which phase change occurred and subsequently the temperature was recorded. Based on the observed Tmf and Th the density of the fluid was calculated by including these values in the equations of state for fluids of known composition of system under observation. The calculated values of bulk densities were further validated by modeling the observed Tmf and Th by using computer package FLUIDS (Bakker, 2003). The package FLUIDS deals with the fluid components such as H_2O, CO_2, CO, H_2, O_2, CH_4, N_2, C_2H_6, H_2S, NH_3, and the salt constituents viz. NaCl, KCl, $CaCl_2$, $MgCl_2$. Further, salt constituents dissolved in water in the form of corresponding anions and cations, i.e. Na+, K+,Ca^{2+}, Mg^{2+} and Cl^- were analysed. The package consists of five main groups of programs, developed on DOS-based platforms: BULK, ISOC, TEST, Loner and Aqso. Thereafter, the detailed compositions of the inclusions were determined using micro-Raman spectroscopy to achieve an appropriate confirmation of paleo-fluid compositions. Furthermore, on the basis of above observations the temperature, pressure and depth of entrapment of the inclusions were determined. In the present study the minute size of inclusions does not permit to identify the eutectic temperature. Therefore, Tf, Tfim and Th, were

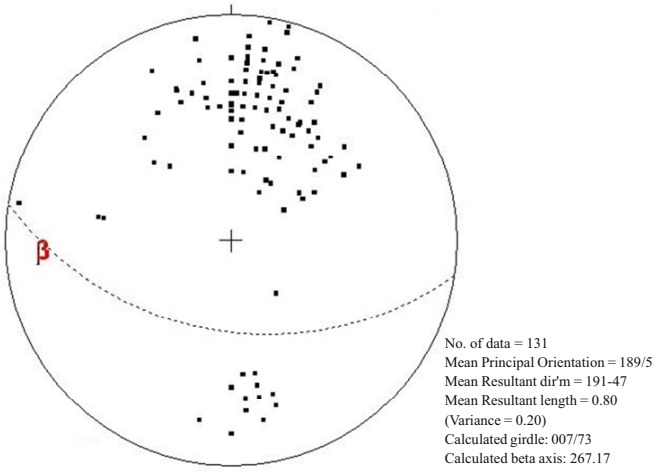

Fig.8. Showing the poles of foliations in the study area

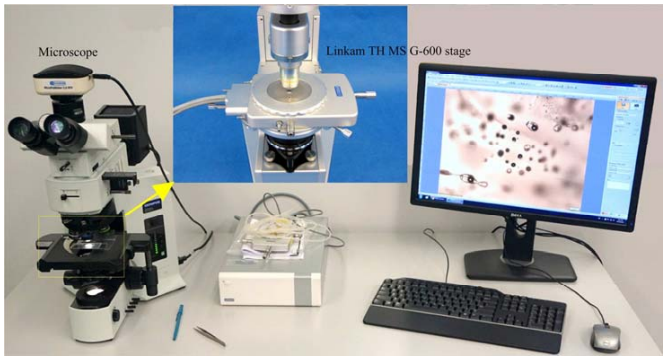

Fig.9. View of thermometric analysis instruments

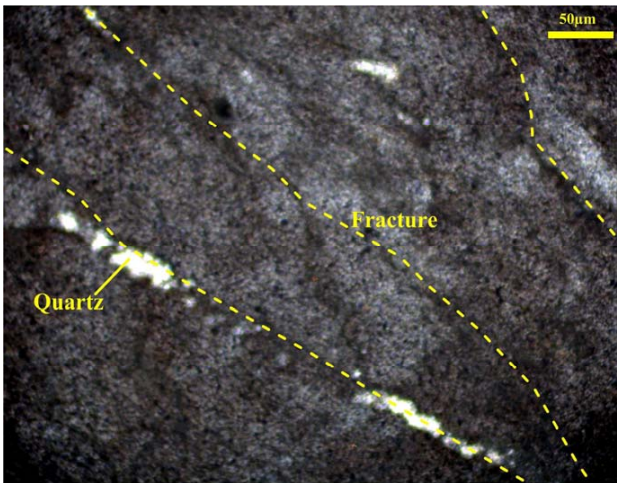

Fig.10. Microphotograph of quartz vein PR 4, near Fafrakund locality, Sonbhadra, Uttar Pradesh.

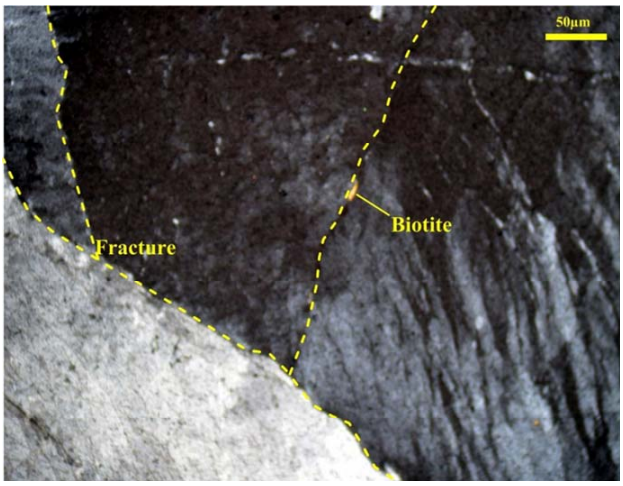

Fig.11. Microphotograph of quartz vein PR 5, near Fafrakund locality, Sonbhadra, Uttar Pradesh

measured mostly on the same fluid inclusions under well-equipped high resolution facilities. The heating and freezing of fluid inclusions were performed at a minimum cooling/heating rate of five degree per minute and at a maximum rate of 20°C per minute. The micro-thermometric data were collected primarily from fluid inclusions having consistent volumetric liquid-vapor ratios. Generally, the composition of the inclusions can be determined in three ways; firstly from first melting temperature (marked by first bubble movement, i.e. the eutectic temperature), secondly from laser micro-Raman spectroscopy and finally from physically crushing the inclusions and analyzing them chemically. In present study laser micro-Raman spectroscopy was used to determine the composition of inclusions. The laser micro-Raman spectroscopy is a recent advance in fluid inclusion studies which characterizes and quantitatively estimates the amount of molecular species present in fluids. Raman spectroscopy is used for analysis of materials in inclusions and provides an efficient, non-destructive and sensitive tool for an assessment of fluid inclusions composition and estimation of the pressures (e.g., Wopenka et al., 1990; Burke, 2001, Rosso et al., 1995; Yamamoto et al., 2006; 2007).

Petrography of Fluid Inclusion

The petrography of selected quartz veins suggests deformed nature of quartz vein with multiple sets of fractures (Fig. 10-11). The petrographic wafers contain mainly biphase (L+V) aqueous inclusions in which the liquid inclusions are found more in numbers. They are mostly primary in nature (except few secondary inclusions) since they occur along the growth zones and isolated planes of the quartz (e.g. Roedder, 1984). Geometrically, the fluid inclusions exhibit various shapes viz. rectangular, rhombic, elongated, oval, and irregular and range in sizes from 8 to 16 microns, where majority of inclusions have sizes of more than 10 micron (Fig.12). In visual estimations, the degree of fill in inclusions ranges from 80 to 90% fluid by volume where some of the primary inclusions show 'Brownian motion'. The secondary fluid inclusions are found oriented along the fractures having their longer side parallel to the general fracture system. Such orientation along the healed fractures of quartz indicate their origin under brittle deformation (e.g.Wilkins and Barkas, 1978) (Fig.10).

RESULTS AND DISCUSSION

The foliations present in phyllitic rocks strike E-W direction and are showing steep dip in southern direction and even vertical at some places. The trend and pattern of foliations present in phyllitic rocks show a good correlative relationship with the major tectonic trend of

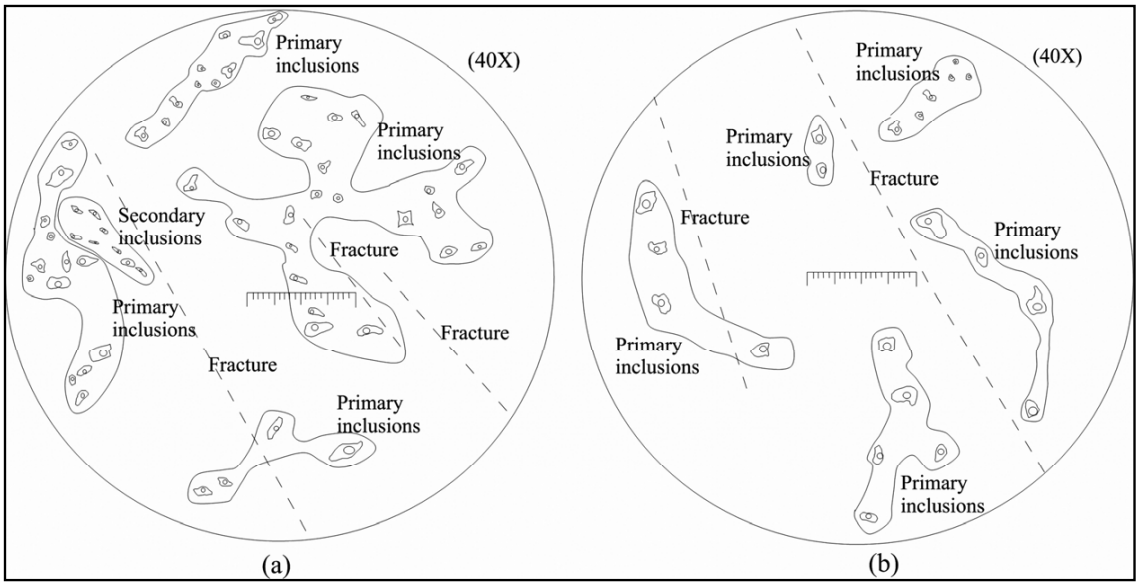

Fig.12. Representative populations of primary and secondary inclusions in samples (a) PR-4 and (b) PR-5

northern block of CITZ (Acharyya, 2003) (Fig.3). The exposures of quartz veins are mainly emplaced in phyllitic rocks and are also oriented parallel or slightly oblique to the strike of foliation. The quartz veins in the area are aligned in a linear trend. These reveal the resultant maximum principal stress which has compressed the rock from north to south direction and responsible for the generation of weak planes along which the silica rich solution got emplaced and resulted in the formation of massive quartz vein found throughout the area.

The fluid inclusions in these quartz veins are mainly bi-phase aqueous in nature and occur as isolated populations (Fig.12). The primary fluid inclusions of euhedral rectangular, rhombic, elongated, oval, and irregular shapes and the sizes range from 8 to 16 micrometer (μm), with majority of inclusions having sizes more than 10 micron (Fig.12). These suggest the formation of variable shaped spaces and geometries due to differential behaviour of host rocks under variable stress conditions. The analogous degree of fill in fluid inclusions at room temperature regardless the sizes of the primary inclusions suggest that the fluids were trapped as single phase liquid which got separated into two phases with decrease in temperature (Nishimura et al., 2008).

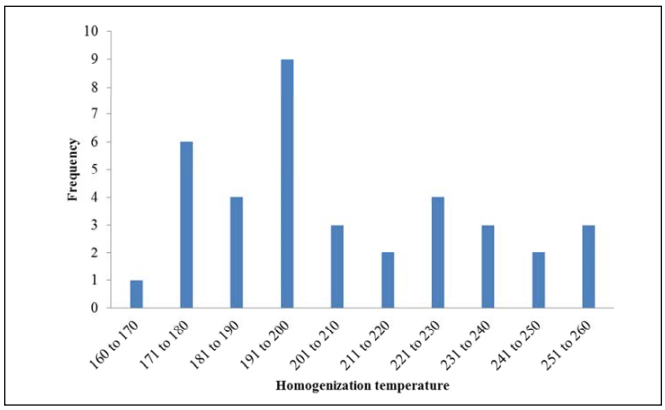

Fig.13. Frequency distribution of homogenization temperatures.

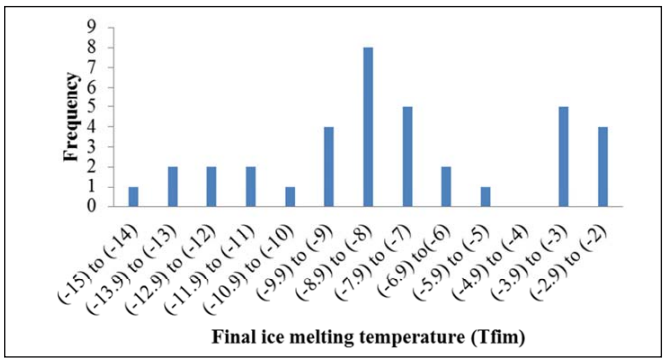

Fig.14. Frequency distribution of final ice melting temperatures.

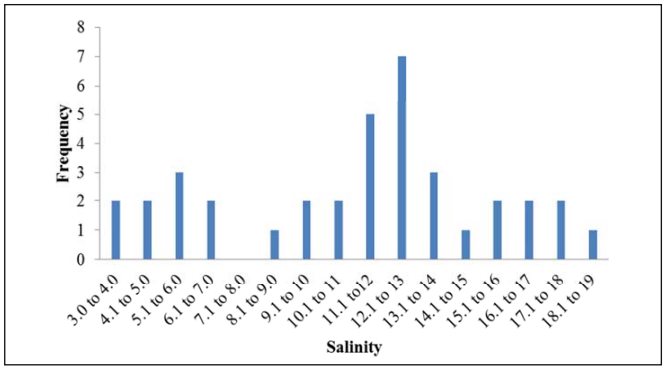

Fig.15. Frequency distribution of salinity in wt% NaCl

Therefore, the homogenization temperatures are considered to be minimum temperatures of fluid entrapment and host mineral formation (e.g. Roedder, 1984). The homogenization temperatures of inclusions in quartz vein of the Parsoi Formation range from 168.8°C to 256.3°C with an average of 205.55°C. The frequency distributions of inclusions with respect to their homogenization temperatures exhibit unimodal distribution where the primary modes occur at temperature range 190-200°C (Fig.13). The low variation in degree of fill also suggests absence of boiling of the fluids at the time of their trapping. The aqueous inclusions having melting temperatures (Tfim) below 0.0°C, is an indicator of presence of salts in inclusions. The final ice melting temperature range from -14.6°C to -2.2°C with an average of about -7.87°C, hence suggests the saline nature of inclusions. The frequency distributions of fluid inclusions with respect to ice melting temperatures show unimodal distribution and primary modes occur at temperature range between -8.9°C to -8°C (Fig.14). The above observations suggest compositions of fluid inclusions in the H_2O-NaCl system. The higher final melting temperature suggests low internal pressure (e.g. Goldstein and Reynolds, 1994). In view of the values of Tfim and Th the determined densities of the fluid ranges between 0.85 to 1.084334 g/cc (after Archer, 1992) which indicate comparatively low fluid density. The salinities of the inclusions ranges from 3.7 to 18.29 wt. % NaCl equivalent with an average of 11.19 wt. % NaCl and shows a distinct unimodal distribution with peaks at 12–13 wt. % NaCl equivalents which indicate the presence of a fluid of low to intermediate salinity (Fig.15, Table.2). The salinity data correlated with the similar works done by Wilkinson, (2001), Tun et al., (2014) show good correlation. Petrographically the veins shows the absence of daughter crystals in the aqueous inclusions and the calculated salinity of the inclusions are in support of the observations made by Bodnar and Vityk, (1994). The presence of low salinity to moderate salinity fluid, absence of daughter mineral, lacking of gas, and salinity versus homogenization temperature plot suggests that the inclusions in the quartz veins are of epithermal in nature (Fig.16). The plot suggests that the basic properties of the fluid involved in the formation of the inclusions are confined within halite saturation curve and critical curve of pure NaCl solution. Therefore, these inclusions may have formed from modified surface

Table 2. Fluid inclusion data of samples PR-4 and PR-5

Sample No. PR-4				Sample No. PR-5			
Tf	Tfim	TH	Salinity	Tf	Tfim	TH	Salinity
-38.2	-9.7	171.2	13.61558	-43.1	-3.9	179.2	6.302759
-56.1	-8.4	187.5	12.16338	-42.7	-3.6	177.6	5.861155
-55.9	-13.6	191.2	17.43388	-53.6	-8.9	232.9	12.73359
-59.4	-11.5	192.5	15.47168	-46.7	-11.3	254.4	15.2738
-43.5	-5.4	172.2	8.410835	-43.1	-6.3	205.7	9.598978
-44.3	-6.3	205.7	9.598978	-37.8	-8.1	195.2	11.81405
-52.4	-8.5	232.9	12.27862	-39.5	-7.9	191.3	11.5781
-48.7	-12.2	254.4	16.1487	-55.1	-9.5	245.3	13.39851
-46.1	-10.4	192.2	14.35788	-52.1	-9.1	235.2	12.95754
-37.8	-8.8	195.2	12.62073	-50.7	-2.8	221.7	4.649699
-48.3	-7.9	196.7	11.5781	-49.4	-14.6	256.3	18.29979
-55.8	-7.6	224.2	11.21952	-39.6	-8.2	193.7	11.9311
-44.3	-3.7	216.5	6.009116	-46.8	-7.4	197.3	10.97732
-53.2	-7.3	188.6	10.85526	-87.9	-12.8	173.7	16.71039
-56.5	-8.9	240.8	12.73359				
-59.3	-9.6	168.8	13.50733				
-52.2	-2.3	219.8	3.866959				
-89.6	-13.9	171.3	17.69801				
-41.8	-3.9	185.2	6.302759				
-37.9	-2.9	183.1	4.803863				
-44.7	-2.2	223.9	3.708003				
-52.3	-3.1	222.9	5.109832				
-46.2	-8.7	209.4	12.50729				

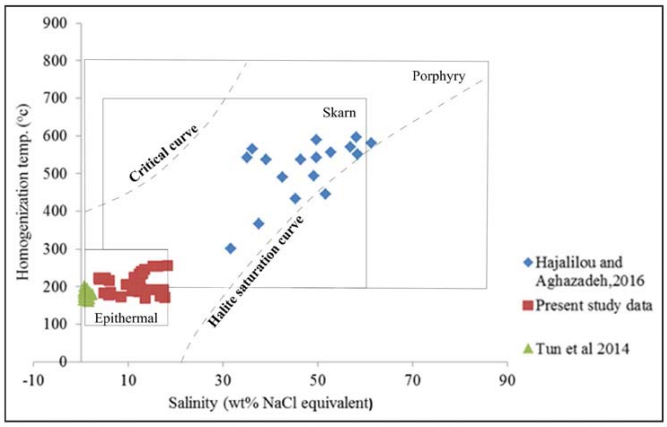

Fig.16. The variation of homogenization temperature with respect to salinity (Hajalilou and Aghazadeh, 2016).

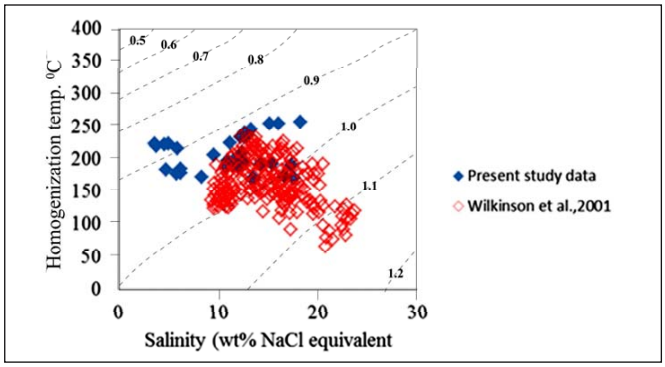

Fig.17. The pattern of homogenization temperature with respect to salinity showing contoured density.

driven fluids which have undergone circulation to a range of depth within the crust of brittle nature exhibiting higher permeability and heat flow (e.g.Wilkinson, 2001). The 'Th' versus salinity plot is having contour lines of constant fluid density (e.g. Bodnar, 1983) which suggest the low density fluids and density driven flow mechanism (Fig.17). The epithermal nature of the inclusions reveals involvement of low trapping pressures and therefore, the temperatures of formation of quartz veins can be estimated from the range of homogenization temperatures which are the histogram mean of homogenization temperatures (Wilkinson, 2001; Tun et al., 2014) (Fig.13). The palaeo depth of quartz vein formation is estimated to be around 200 m on the basis of assumption of hydrostatic pressure (after Haas, 1977) (Fig.18).

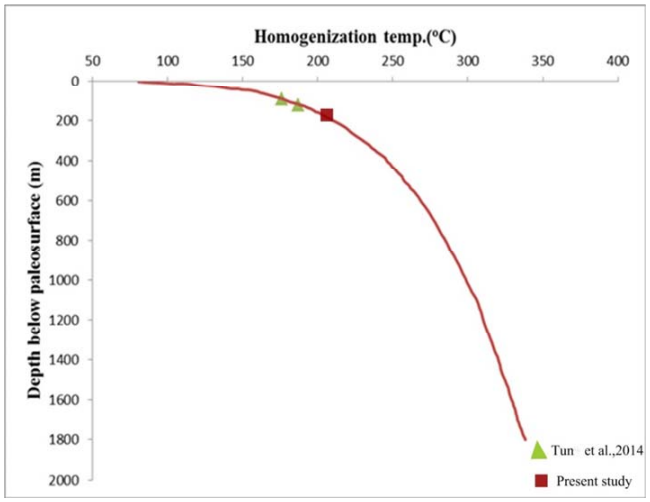

Fig.18. Estimation of palaeo-depth for entrapment of fluid in quartz veins (after Haas, 1971).

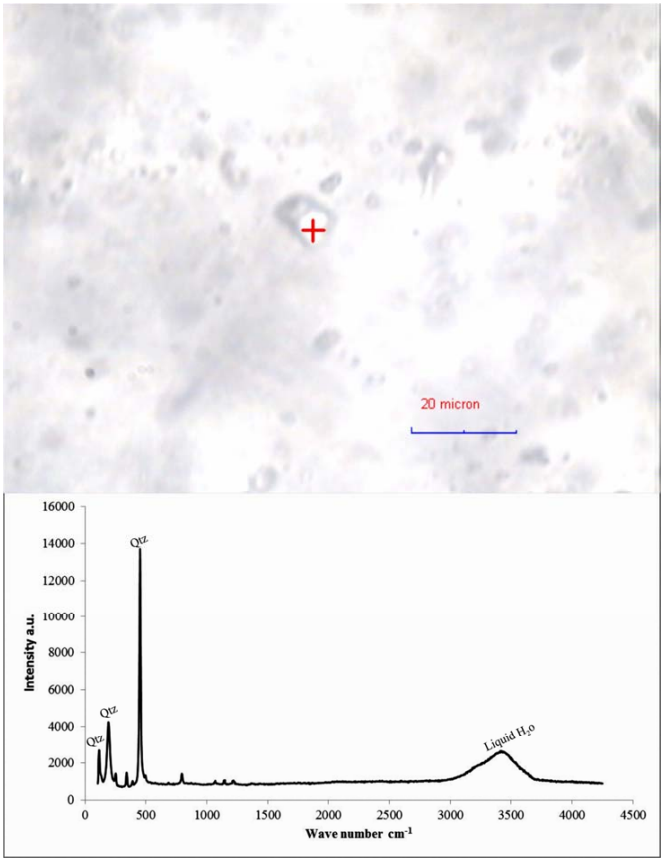

Fig.19. Shape of fluid inclusions and Micro-Raman spectra (sample PR-4)

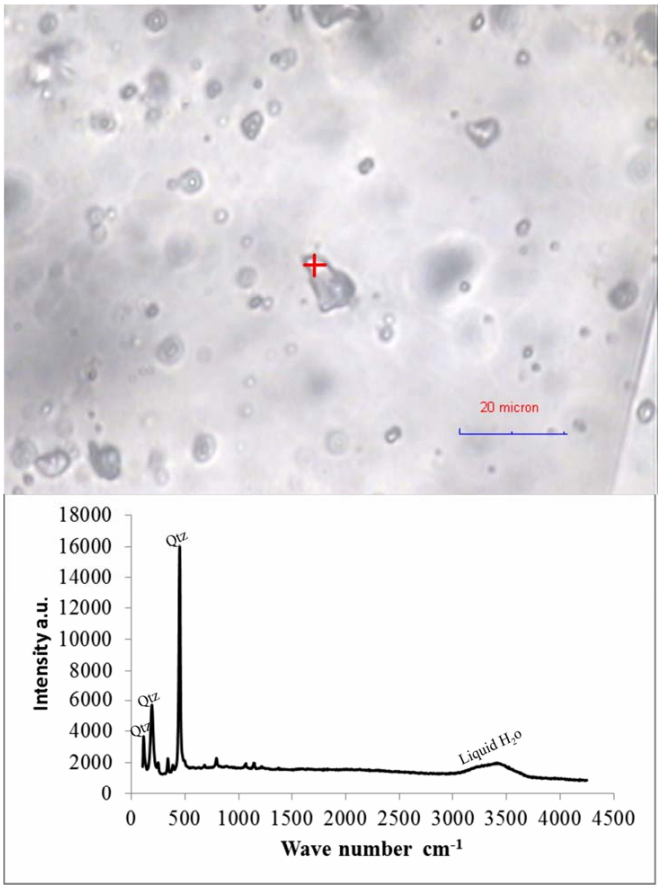

Fig.20. Shape of fluid inclusions and Micro-Raman spectra (sample PR-5)

At this depth the dominating fluid pressure is close to hydrostatic pressure (Equation.2) :

$$P = \rho \times g \times d \quad (2)$$

where, ρ = fluid density; g = acceleration due to gravity; d = depth

The hydrostatic pressures calculated by the equation is found to be in the range of 1.666 to 2.125 kbar.

The bulk fluid compositions determined by using equation of state given by Bodnar and Vityk, (1991), Knight and Bodnar, (1989) are found in the order of $x(H_2O) = 0.923732$, $x(Na^+) = 0.038134$, $x(Cl^-) = 0.038134$. The micro-Raman analysis of primary inclusions suggests that the water fill in the inclusions are of comparatively moderate to low salinity. The Raman spectra indicates no trace of other gases viz. H_2, C_2H_2, C_2H_4, C_6H_6, H_2S and CO, etc. as well as SO_4^{2-} and HCO_3 ions. The spectra exhibit three peaks of quartz at 114 cm^{-1}, 190 cm^{-1} and 452 cm^{-1} (strongest peak). Further the spectra exhibits peaks in the form of broad band of several hundred cm^{-1} and shows maximum peak at 3390 cm^{-1} which suggests liquid water encages in fluid inclusions (e,g, Dubessy *et al*.,1992; Frezzotti et al., 2012) (Fig.19-20).

CONCLUSION

The study concluded the general EW trending and southerly dipping steep foliations corresponds to characteristic tectonic trend of northern block of CITZ of Parsoi Formation exposed in and around Parsoi village, central India. The quartz veins are oriented parallel or slightly oblique to the strike of foliation and showed linear trend due to orientation of maximum principal stress acting in north-south direction. The impact of such maximum principal stress is responsible for generation of weak planes and fractures. The weak planes and fractures have facilitated the emplacements of silica rich solution in foliated rocks and formation of massive quartz vein in the area. These veins contain inclusions of varied shapes and minute sizes (ranging from 8 to 16 microns) due to narrow and small spaces available in emplaced veins. The inclusions are liquid rich and having relatively homogeneous degree of fill (ranging from 80 to 90 percent) where some of them are showing Brownian motion. The preferred orientation of minute secondary inclusions favours their post-brittle deformation entrapment in quartz veins. The homogenization temperatures of fluid inclusions ranged between 168.8°C to 256.3°C (average = 205.55°C) and final ice melting temperature are recognized from -14.6°C to -2.2°C (average = -7.87°C). The fluids entrapped in the inclusions are aqueous saline in nature (H_2O-NaCl) having moderate to low salinity (3.7 to 18.29wt% NaCl equivalent.), low density (0.85 to 1.084334 g/cc) and low internal pressure and got entrapped in absence of boiling condition and favoured density driven mechanism. The fluid inclusions are composed of liquid H_2O only entrapped between pressure 1.666 to 2.125 kbar at depth of 200m. Overall the evidences are in support of epithermal nature of fluid inclusions. The lithological associations, nature of structural features, and fluid inclusions and their entrapment conditions in the case of present study area correlated with other known epithermal deposits of gold may be helpful in exploring the potential zone of gold mineralization in other area of similar nature too.

Acknowledgement: The authors gratefully acknowledge Prof. H.S. Pandalai for his constant support and for providing laboratory facility in Department of Earth Science, IIT Bombay. The authors are thankful for the financial assistance provided by the University Grants Commission, New Delhi and Department of Atomic Energy (BRNS), Mumbai in form of research project (File No.1038/2012 (SR) and (2013/36/56-BRNS/2447). The authors are thankful to the Director, Indian Institute of Technology (Indian School of Mines), Dhanbad-826 004.

References

Acharyya, S.K. and Roy, A. (2000) Tectonothermal history of the Central Indian Tectonic Zone and reactivation of major faults/shear zones. Jour. Geol. Soc. India, v.55, pp.239–256.

Acharyya, S.K. (2003) The nature of Mesoproterozoic Central Indian Tectonic Zone with exhumed and reworked Older Granulites, Gondwana Res., v.6(2), pp.197-214

Archer, D.G. (1992) Thermodynamic properties of the NaCl +H_2O system: II. Thermodynamic properties of NaCl(aq), NaCl $2H_2O$(cr), and phase equilibria, Jour. Phys. Chem. Ref. Data, v.28, pp.1-17.

Bakker, R.J. (2003) Package FLUIDS 1. Computer programs for analysis of fluid inclusion data and for modelling bulk fluid properties. Chem. Geol., v.194, pp.3-23.

Bodnar, R.J. and Vityk, M.O. (1994) Interpretation of micro thermometric data for H_2O-NaCl fluid inclusions: Fluid Inclusions in Minerals, Methods and Applications, Vivo, B.D. and Frezzotti, M.L., (Eds.), published by Virginia Tech, Blacksburg, VA, pp.117-130.

Bodnar, R.J. (1985) Pressure-volume temperature-composition (PVTX) properties of the system H_2O-NaCl at elevated temperatures and pressures, Unpub. Ph.D. Dissertation, The Pennsylvania State Univ, University Park, PA, pp.183.

Bodnar, R.J. (1993). Revised equation and table for determining the freezing point depression of H_2O-NaCl solutions. Geochim. Cosmochim. Acta., v.57, pp.683-684.

Bodnar, R.J. (2003) Introduction to aqueous fluid systems. *In:* I. Samson, A. Anderson, and D. Marshall (Eds.), Fluid Inclusions: Analysis and Interpretation. Mineral. Assoc. Canada, Short Course, v.32, pp.81-99.

Bodnar, R.J. (2003) Re-equilibration of fluid inclusions: In I. Samson, A. Anderson, and D.Marshall, eds. Fluid Inclusions: Analysis and Interpretation. Mineral. Assoc. Can., Short Course Ser., v.32, pp.213-230.

Burke, E.A.J. (2001) Raman micro spectrometry of fluid inclusions, Lithos, v.55, pp.139–158.

Chi, G. and Guha, J. (2011) Microstructural analysis of a subhorizontal gold-quartz vein deposit at Donalda, Abitibi greenstone belt, Canada: Implications for hydrodynamic regime and fluid-structural relationship, Geoscience Frontiers, v.2(4), pp.529-538.

Crawford, M.L., (1992). Fluid inclusions -What can we learn? Earth Sci. Rev., v.32, pp.137-139.

Dubessy, J., Boiron, M.C., Moissette, A., Monnin, C. and Stretenskaya, N. (1992) Determination of water, hydrates and pH in fluid inclusions by micro-Raman spectrometry. European Jour. Min, v.4, pp.885–894.

Frezzotti, M.L., Tecce, F. and Casagli, A., (2012) Raman spectroscopy for fluid inclusion analysis. Jour. Geochem. Exp., v.112, pp.1–20.

Ghosh, A. 1966) On the geology and structure of the Pre-Vindhyan rocks around Parsoi and Kunwar in parts of Mirzapur District, U.P. Geol. Surv. India, Unpubld. Report, pp.1-27.

Goldstein, R.H. and Reynolds, T.J. (1994) Systematics of fluid inclusions in diagenetic minerals. Soc. Sed. Geol., Short Course, v.31, pp.199.

Haas, J.L., Jr. (1971) The effect of salinity on the maximum thermal gradient of a hydrothermal system at hydrostatic pressure. Econ. Geol., v.66, pp.940–946.

Hajalilou, B., and Aghazadeh, M. (2016) Fluid inclusion studies on quartz veinlets at the Ali Javad Porphyry Copper (Gold) Deposit, Arasbaran, Northwestern Iran, Jour. Geosci. Environ. Prot., v.4, pp. 80-91.

Hollister, L.S. and Crawford, M.L. (1981) Fluid inclusions: Applications to petrology. Min. Assoc. Canada, v.6, pp.278-304.

Iqballudin, and Mohgni, A. (1981) Stratigraphy of the Bijawar Group in Son Valley, Mirzapur district and Sidhi district, M.P. Geol. Surv. India Spec. Publ. pp.381–93.

Kant, W., Warmada1, I.W., Idrus, A., Setijadji, L.D. and Watanabev, K. (2012) Fluid inclusion study of the polymetallic epithermal quartz veins at Soripesa prospect area, Sumbawa island, Indonesia, Jour. SE Asian Appl. Geol., v.4(2), pp.77-89.

Knight, C.L. and Bodnar, R.J. (1989) Synthetic fluid inclusions. IX. Critical PVTX properties of NaCl-H_2O solutions, Geochem. Cosmochim. Acta, v.53, pp.3-8.

Kumar, G. (2005) Geology of Uttar Pradesh and Uttaranchal. Geol. Soc. India, Bangalore, pp.383.

Mathur, S.M. and Narain, K. (1981) Geosyncinal sedimentation with Archaeans of the Mirzapur-Sidhi area. Geol. Surv. India Spec. Publ., v.3, pp.31–37.

Mehrabi, B., Siani, M. G., Goldfarb, R., Azizi, H., Ganerod, M. and Marsh,

E.E. (2016) Mineral assemblages, fluid evolution, and genesis of polymetallic epithermal veins, Glojeh district, NW Iran, Ore Geol. Rev., v.78, pp.41-57.

Moncada, D. and Bodnar R.J. (2012) Gangue mineral textures and fluid inclusion characteristics of the Santa Margarita Vein in the Guanajuato Mining District, Mexico. Cent. European. Jour. Geosci., v.4(2) pp.300-309.

Morales, A., Vivallo, W. and Darce, M. (1993) Fluid inclusion studies of epithermal gold-bearing quartz veins in the La Liberted district, Nicaragua, Rev. Geol. Amer. Central, v.16, pp.23-38.

Nair, K.K.K., Jain, S.C. and Yedekar, D.B. (1995) Stratigraphy, Structure and Geochemistry of the Mahakoshal greenstone belt. Mem. Geol Soc. India, no.31, pp.403-432.

Nishimura, K., Amita, K., Ohsawa, S., Kobayashi, T. and Hirajima, T. (2008) Chemical characteristics and trapping P-T conditions of fluid inclusions in quartz veins from the Sanbagawa metamorphic belt, SW Japan. Jour. Mineral. Petrol. Sci., v.103, pp.94–99.

Radhakrishna, B.P. (1989) Suspect tectono-stratigraphic terrain elements in the Indian subcontinent. Jour. Geol. Soc. India, v.34, pp.1–24.

Randive, K.R., Hari, K.R., Dora, M.L., Malpe, D.B. and Bhondwe, A.A. (2014) Study of fluid inclusions: methods, techniques and applications, Gondwana Geol. Magz., v.29(1-2), pp.19-28.

Ravi Shanker (1993) Structural and geomorphological evolution of 'SONATA' rift-zone in central India in response of Himalayan uplift. Jour. Palaeontol. Soc. India, v.38, pp.17–30.

Roedder, E. (1968) Temperature, salinity, and origin of the Ore-forming fluids at pine point, Northwest Territories, Canada, from fluid inclusion studies, Soc. Econ. Geologists, v.63(5), pp.439-450.

Roedder, E. (1984) Fluid Inclusions. Min. Soc. Amer. Rev. in Min., v.12, pp.644.

Roedder, E. (1992) Optical microscopy identification of the phases in fluid inclusions in minerals. The Microscope, v.40, pp.59-79.

Roedder, Edwin and Bodnar, R.J. (1980) Geologic pressure determinations from fluid inclusion studies. Ann. Rev. Earth Planet. Sci., v.8, pp.263-301.

Ronald, W.T., Wilkins, J., and Barkas, P. (1978) Fluid inclusions, deformation and recrystallization in granite tectonites, Contrib. Mineral. Petrol., v.65(3), pp.293–299.

Rosso, K.M. and Bodnar, R.J. (1995) Micro thermometric and Raman spectroscopic detection limits of CO_2 in fluid inclusions and the Raman spectroscopic characterization of CO_2. Geochem. Cosmochim. Acta, v.59, pp.3961–3975.

Roy, A. and Devarajan, M.K.(2000) Appraisal of the stratigraphy and tectonics of Proterozoic Mahakoshal Supracrustal belt, central India. Geol. Surv. India Spec. Publ., no.57, pp.79–97.

Roy, A. (2008) Magma emplacement in Central Indian Tectonic Zone – An evidence for large scale crustal growth and recycling during Proterozoic: A review; National Symposium on Geodynamics and evolution of Indian Shield – through time and space (Golden Jubilee of the Geol. Soc. India at Centre for Earth Science Studies, Thiruvananthapuram, pp.1–2.

Simeone, R. and Simmons, S.F. (1999) Mineralogical and fuid inclusion studies of low-sulfidation epithermal veins at Osilo (Sardinia), Italy, Mineralium Deposita, v.34, pp.705-717.

Sorby, H.C. (1858) On the microscopic structure of crystals, indicating the origin of minerals and rocks. Geol. Soc. London Quart. Jour., v.14(1), pp.453-500.

Srivastava, A.K. (1969) A petrochemical study of the Jhirgadandi aureole rocks district Mirzapur, Uttar Pradesh, India. Jour. Geol. Soc. India, v.4, pp.82–93.

Srivastava, A.K., Kumar, H., Ravi Shankar and Kumar, G. (2000b) Observations on mafic and microgranular enclaves hosted in Jhirgadandi pluton, Sonbhadra district, Uttar Pradesh. Geosci. Jour., v.31, pp.139–146.

Srivastava, A.K., Kumar, H.P. and Kumar, G. (2000a) Geochemical characteristics of the Jhirgadandi granitoid, Sonbhadra district, Uttar Pradesh; *In:* Gyani, K.C. and Kataria, P. (Eds.), Proc. National Seminar on Tectonomagamatism, Geochemistry and Metamorphism of Precambrian Terrains, Univ. Dept. Geol. Udaipur, pp.189–199.

Tun, M.M., Warmada, I.W., Idrus, A., Harijoko, A., Verdiansyah, O. and Watanabe, K. (2014) Fluid inclusion studies of the epithermal quartz veins from Sualan prospect, west Java, Indonesia, Jour. SE Asian Appld. Geol., v.6(2), pp.62–67.

Woods, T.L., Roedder, E. and Bethke, P.M. (1982) Fluid-inclusion data on samples from Creede, Colorado, in relation to mineral paragenesis, United States Department of the Interior Geological Survey, pp.82-313.

Wopenka, B., Pasteris, J.D. and Freeman, J.J. (1990) Analysis of individual fluid inclusions by Fourier transform infrared and Raman micro-spectroscopy, Geochim. Cosmochim. Acta, v.54, pp.519-533.

Yamamoto, J., Kagi, H., Kawakami, Y., Hirano, N., and Nakamura, M. (2007) Paleo-Moho depth determined from the pressure of CO_2 fluid inclusions: Raman spectroscopic barometry of mantle- and crust-derived rocks, Earth and Plan. Sc. Lett., v.253, pp.369–377.

Yamamoto, J., and Kagi, H. (2006) Extended micro-Raman densimeter for CO_2 applicable to mantle-originated fluid inclusions, Chem. Letter, v.35, pp.610–611.

(Received: 17 November 2016; Revised form accepted: 20 February 2017)